International Symposium
On Turbulence and Shear Flow
Phenomena (TSFP-9)
June 30 - July 3, 2015 *Melbourne, Australia*

DYNAMIC ESTIMATION OF VORTEX SHEDDING

Simon J. Illingworth
Department of Mechanical Engineering, University of Melbourne, VIC 3010, Australia
sillingworth@unimelb.edu.au

ABSTRACT

This paper considers the estimation of a flow field using only information from a single time-resolved sensor. We call this the estimation problem, and it is closely related to the feedback control problem since, if one wishes to control a flow with limited measurements available, it is important that one can estimate what is happening in other parts of the flow. Tackling this problem is important not only for feedback control purposes, but also for any situation where one wishes to estimate a flow field using limited measurements. The estimation is performed using a Kalman filter, an estimation tool which is widely used in guidance, navigation and control, as well as in signal processing. The Kalman filter uses dynamic (i.e. time-resolved) measurements, coupled with a model of a system, to estimate a system's full state. There are two parts to the study. The first part considers the estimation problem for the flow past a cylinder at low Reynolds numbers. We look at the accuracy of the estimate when the single sensor measurement is *i*) a single velocity sensor in the wake (whose location can vary); and *ii*) the lift force on the cylinder. The second part is concerned with how well the estimation problem can be performed. To do this we consider the Ginzburg-Landau equation, a well-known model system which displays many of the phenomena seen in fluid systems. This allows us to quantify the efficacy of the estimator as the measurement type and the disturbance characteristics vary.

INTRODUCTION

The von Kármán vortex street in the two-dimensional cylinder wake first appears at a Reynolds number near 49 (Williamson, 1996). This vortex street gives rise to increased drag and unsteady lift forces. The advantages of suppressing these vortices is therefore clear, and the two-dimensional cylinder wake has become a canonical problem in flow control.

This paper aims to address a research question which is closely related to the control problem: the estimation problem. Clearly if one wishes to control a fluid flow using feedback, then one needs to be able to measure salient quantities for that flow. In an ideal world, one would have access to all flow quantities (for example velocities and pressures) at all points in the flow, and in simulations one can do this. In experiments, however, we are limited to those quantities that can actually be measured—and the less intrusive that measurement, the better. This poses a problem: We want to control the flow as a whole, and yet we cannot measure most of the flow.

In previous studies on flow control, the estimation problem is commonly addressed using Linear Stochastic Estimation (LSE), which generates a correlation database between different points in the flow (Adrian *et al.*, 1989; Guezennec, 1989). One then uses this correlation database to estimate the flow at a particular point using known, measured data at another point. Linear Stochastic Estimation is a useful tool and has been used for a range of flows. However, LSE is not a *dynamic* estimation technique: it makes use only of instantaneous measurements (i.e. a 'snapshot' of the available measurements), but does not make use of the time history of those measurements.

The utility of time-resolved, dynamic measurements for estimation is well-understood and often exploited in other fields. The Kalman filter (Kalman, 1960)—which is widely used in guidance, navigation and control, as well as in signal processing—is a wonderful example of how dynamic measurements, when coupled with a model of a system, can be used to estimate the system's full state (which may be of much larger dimension than the measurements available). The Kalman filter uses a linear model of the system to be estimated, but nonlinear extensions have been developed, including the extended Kalman filter (Anderson & Moore, 1979) and the unscented Kalman filter (Julier & Uhlmann, 2004). The Kalman filter has been applied to problems in fluid mechanics in a small number of previous studies including low-Reynolds-number turbulence (Hœpffner *et al.*, 2005); compressible cavity oscillations (Rowley & Juttijudata, 2005) and a transitional flat-plate boundary layer (Guzmán Iñigo *et al.*, 2014).

This paper looks at estimating an entire flow field using only information from a single time-resolved sensor for two systems: the flow past a cylinder at $Re = 45$; and the Ginzburg-Landau equation (to be described). The estimation is performed using a Kalman filter. Tackling this problem is important not only for feedback control purposes, but also for any situation where one wishes to estimate an entire or partial flow field using limited measurements.

The paper is organized as follows. The estimation problem is first stated, and the structure of a dynamic estimator is explained. Dynamic estimation is then applied to the flow past a cylinder at a Reynolds number of 45. Excellent results are seen—both when a single velocity measurement in the wake is used, and when only the lift force on the cylinder is measured. This is followed by the application of a dynamic estimator to the Ginzburg-Landau equation, a relatively well-studied model system which displays many of the phenomena seen in fluid systems. This allows us to precisely quantify the efficacy of the estimator as the disturbance characteristics and measurement type vary, providing important information concerning the estimation problem for fluid flows. The paper finishes with conclusions.

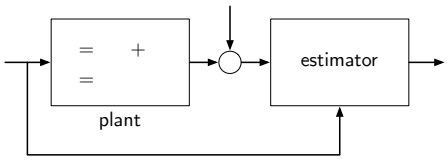

Figure 1. An estimator uses the system input, u, and the output, y, to generate an estimate of the state, $\hat{x}$.

DYNAMIC ESTIMATION AND THE KALMAN FILTER

We are interested in estimating the full state of a state-space model of the form

$$\dot{x}(t) = Ax(t) + B_u u(t) + B_w w(t) \tag{1a}$$
$$y(t) = Cx(t) + n(t), \tag{1b}$$

where $u \in \mathbb{R}^{p_u}$ is a vector of inputs; $w \in \mathbb{R}^{p_w}$ is a vector of unknown disturbances; $y \in \mathbb{R}^q$ is a vector of outputs; $n \in \mathbb{R}^q$ is sensor noise; $x \in \mathbb{R}^n$ is the system state; and A, B_u, B_w and C are suitably-dimensioned matrices. For the cylinder, this state-space model is found by applying system identification to input-output data from direct numerical simulations. For the Ginzburg-Landau equation, it is formed directly from the discretization of the governing equation.

Two sources of unknown exogenous inputs are included in the state-space model (1). The first is sensor noise, $n(t)$, which contaminates the sensor measurements so that the measured value, $y(t)$ differs from the true value. The second is exogenous disturbances, $w(t)$, which act as an additional input which, by their nature, are unknown.

The estimation problem can then be stated as follows: Given measurements, $y(t)$ (which have been contaminated by noise $n(t)$), together with knowledge of the input, $u(t)$, generate an estimate of the entire system state, $\hat{x}(t)$. For a state-space model of the form (1), a dynamic estimator — which is also often referred to as an *observer* — uses knowledge of $u(t)$ and $y(t)$ to determine an estimate of the full state, $\hat{x}(t)$, and of the output, $\hat{y}(t)$, using

$$\dot{\hat{x}}(t) = A\hat{x}(t) + Bu(t) - L[\hat{y}(t) - y(t)] \tag{2a}$$
$$\hat{y}(t) = C\hat{x}(t). \tag{2b}$$

This system mimics the original state-space model (1), but is also forced by the output error $[\hat{y}(t) - y(t)]$ via the observer gain matrix L. The structure of the estimator is shown in figure 1. Defining an error vector, $e(t) = \hat{x}(t) - x(t)$, (1) and (2) can be combined to give

$$\dot{e}(t) = \dot{\hat{x}}(t) - \dot{x}(t) = (A - LC)e(t) + Ln(t) - B_w w(t). \tag{3}$$

From (3) we see that the error dynamics are determined by the matrix $(A - LC)$, and can therefore be chosen via suitable choice of the observer gain matrix L.

We use a specific type of observer: the Kalman filter, which amounts to a particular choice of the observer gain matrix L. This choice of L is optimal in the sense that the error, $e(t)$ converges in the presence of the stochastic disturbances $w(t)$ and measurement noise $n(t)$, which are each assumed to be zero-mean, Gaussian, white-noise processes.

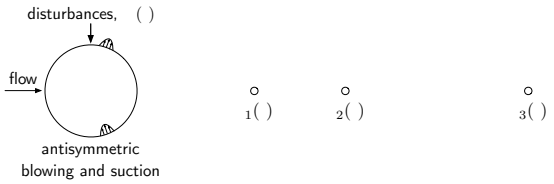

Figure 2. Cylinder arrangement. Disturbances enter at the cylinder surface via randomly-generated antisymmetric blowing and suction. Velocity sensors (○) are positioned 1.75, 2.75 and 4.75 cylinder diameters downstream of its centre. Only one of these sensors is used for estimation.

We will set the input, $u(t)$ to zero both for the cylinder wake and for the Ginzburg-Landau equation. This means that we do not provide any known forcing, and any response of the system is due entirely to the unknown disturbances $w(t)$. Our task can then be thought of as to estimate the effect of the unknown disturbances on the entire flow field, given only knowledge of their effect at a particular point in the flow. (This task is made more challenging by the corruption of the single sensor measurement by sensor noise.)

ESTIMATION OF THE CYLINDER WAKE

We now consider dynamic estimation of the cylinder wake at $\mathrm{Re} = 45$ using only a single sensor measurement. The cylinder flow is solved using direct numerical simulation. The spatial discretization is performed in cylindrical coordinates using an energy-conservative finite-difference scheme (Fukagata & Kasagi, 2002). The code has been validated using grid refinement and boundary placement studies, as well as comparison with experimental data. At Reynolds numbers between 60 and 100, the Strouhal numbers found agree with the experimental parallel-shedding data of Williamson (1989) to within 1 %.

The cylinder arrangement is shown in figure 2. Velocity sensors (which measure the transverse velocity) are positioned $1.75D$, $2.75D$, and $4.75D$ downstream of the cylinder's centre, where D is the cylinder diameter. Only one of these sensors is used for estimation. The flow is perturbed with disturbances introduced at the cylinder's surface which are unknown to the estimator. Our aim is then to use the available sensor measurement (either $v_1(t)$, $v_2(t)$ or $v_3(t)$) to estimate the response of the entire flow field to these unknown disturbances. To perform the estimation problem we first require a suitable reduced-order model. We now consider how this reduced-order model is found.

Reduced-order modelling

A reduced-order model of the wake can be represented in state-space form (1). The Eigensystem Realization Algorithm (ERA) is used to form the reduced-order model (Juang, 1994). The starting point for the ERA is the system's impulse response, which is found in the cylinder's case directly from simulation data. The impulse response (which in this context is also referred to as the system's Markov parameters) is arranged into a particular block data matrix (a Hankel matrix). By factorizing this block data matrix using the singular value decomposition, the state-space matrices in (1) can be found. An important property of the ERA is that it produces reduced-order models which are *balanced*, the balancing referring to the fact that the

observability and controllability Gramians of the reduced-order are equal and diagonal. Physically this means that the input-output behaviour of the system is properly captured, and this is important for feedback control purposes. For more details on the ERA, see Juang (1994), and for its application to flow control, see Ma *et al.* (2009); Illingworth *et al.* (2011).

The dimension of the reduced-order model's output—which is the entire flow field—is very large. There are 220 grid points in the radial direction and 256 grid points in the circumferential direction, which together make for 56,320 output locations. This is not tractable. We might decide to restrict attention to a particular part of the domain, but even then we will have of the order of tens of thousands of outputs. To make the problem tractable, we therefore reduce the number of outputs by computing their leading POD modes. We still use the ERA to find the reduced-order model, and the procedure to find it is then as follows. Perform an impulse response simulation, taking the entire field as the output; compute the leading POD modes of these outputs; and use the time-varying POD coefficients as the output for the ERA. Due to the high dimension of the full field, we use the method of snapshots to compute the POD modes. We use 27 POD modes, which is sufficient to capture 99.99% of the energy in the wake's impulse response. Using the POD coefficients, together with the single sensor, the model has a total of $27+1=28$ outputs. The order of the state-space model (1) provided by the ERA is $n=29$.

Our task now is to estimate the 27 POD coefficients using only values of the velocity at a single sensor. We can achieve this using the dynamic estimator already described. Then at each instant in time, the estimate of the 27 POD coefficients allows us to estimate the entire flow field.

Results

Results at $Re=45$ are now described. We first consider the estimation problem using the transverse velocity at sensor two as the single sensor measurement, and good results are obtained. We then look at the effect of the sensor location on the fidelity of the estimate by considering each of the three sensor locations shown in figure 2 in turn. We do this by considering, for each sensor, the error between the estimated flow and the true flow, integrated in space, and plotted in time. In addition to considering these three velocity sensors, we also consider measuring only the lift force on the cylinder (or rather the coefficient of lift). Excellent results are seen, with the lift measurement providing an estimate which is comparable in accuracy to that given by any of the three velocity sensors.

Estimation with velocity sensor two Estimation of the wake using the transverse velocity at sensor two only is shown in figure 3. Even in the presence of unknown disturbances and measurement noise, the Kalman filter performs remarkably well in estimating the full flow field. This is demonstrated in figure 3 (*a*) as a function of time at the three velocity sensors (only $v_2(t)$ is being used for estimation); and in (*c*,*d*) for a region of the flow at a particular instant in time. Finally, the total perturbation energy as a function of time is also indicated in part (*b*). This perturbation energy is defined as

$$PE(t)=\frac{1}{2}\iint u_T^2(x,y,t)\,\mathrm{d}x\,\mathrm{d}y, \qquad (4)$$

Table 1. $\int\Delta(t)\,\mathrm{d}t$ for each of the four sensing strategies.

sensor	v_1	v_2	v_3	C_L
$\int\Delta(t)\,\mathrm{d}t$	67.1	51.2	28.9	40.1

where u_T is the total velocity perturbation, $u_T=\sqrt{u^2+v^2}$.

Estimation accuracy with varying sensor location and type With excellent results seen for velocity sensor two, it is now interesting to consider what happens as the location of the single sensor is varied: that is, to look at the accuracy of the estimate of the entire flow field for each of the three sensors. This is shown in figure 4 (*a*), which plots the total perturbation energy, $PE(t)$, for each of the three sensor locations, and compares them with the true value. We see that the performance is broadly similar for the three sensors, with the perturbation energy well-estimated in all three cases. The performance of the three sensors is also compared in figure 4 (*b*), which compares the quantity

$$\Delta(t)=\frac{1}{2}\iint[\hat{u}_T(x,y,t)-u_T(x,y,t)]^2\,\mathrm{d}x\,\mathrm{d}y. \qquad (5)$$

That is, the square of the estimation error, integrated in space. From figure 4 (*b*) we see that the three sensors provide estimates which are comparable in accuracy.

It is also interesting to look a more global measurement for estimation. This is achieved in figure 4 by also plotting $\Delta(t)$ when the lift on the cylinder is used as the only sensor measurement. Figure 4 shows that a lift measurement provides an estimate which is comparable with that provided by any of the three velocity measurements.

Table 1 supplements figure 4 by looking at the integral of $\Delta(t)$ with time, $\int\Delta(t)\,\mathrm{d}t$, for the four sensing strategies. This provides a single convenient measure of the estimation error by integrating it in space and time. With this as our measure we see that $v_3(t)$ provides the most accurate estimate, with C_L coming in second place.

Estimation using the lift force With the encouraging results of figure 4 and table 1 in mind, we now

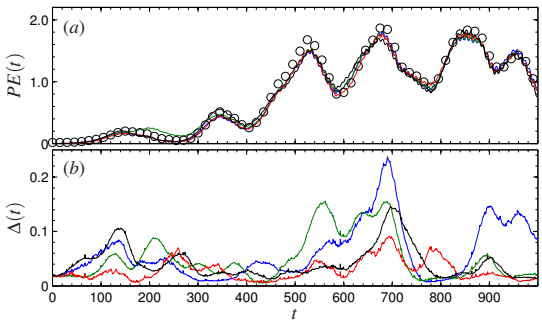

Figure 4. Estimation of the cylinder wake: (*a*) the true total perturbation energy (○) is compared to its estimate using v_1 (blue), v_2 (green), v_3 (red) and C_L (black). In (*b*) the estimation error integrated in space, $\Delta(t)$ (see Eq. (5)), is plotted for the four cases (colours same as in (*a*)).

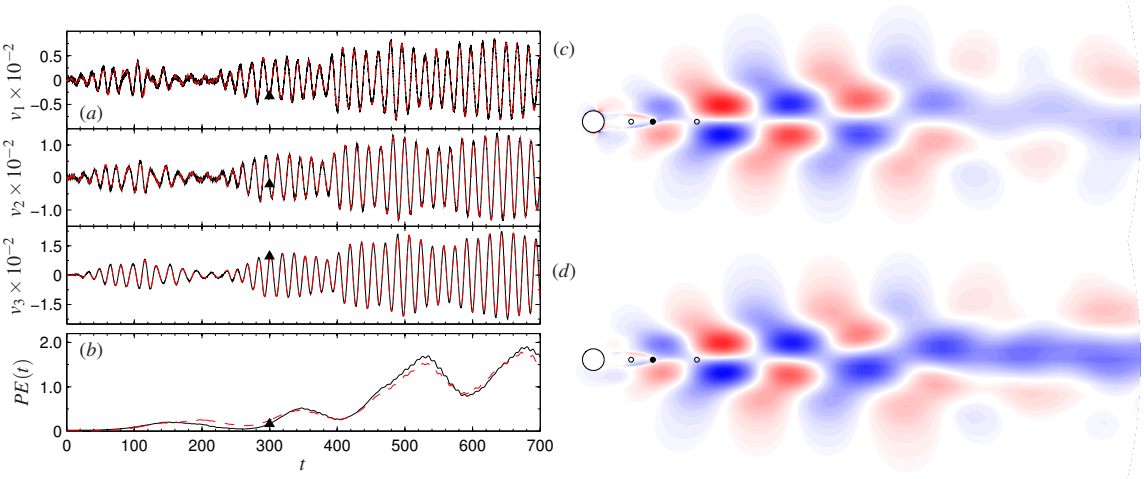

Figure 3. Estimation of the cylinder wake using v_2: (c) the true flow field; and (d) the estimated flow field at a particular instant in time. (a) shows the transverse velocity at the three velocity sensors (indicated in (c,d)). (b) shows the perturbation energy, $PE(t)$. Both the true (—) and estimated values (– –) are shown. The instant shown in (c,d) is indicated by ▲ in (a,b).

repeat figure 3, this time using the lift as the single sensor measurement. This is shown in figure 5 where we see, as expected from figure 4, that measurement of the lift alone provides an excellent estimate of the entire flow field. This is encouraging because it suggests that a surface-based (and therefore more practical) measurement such as lift can provide an estimate which is competitive with that provided by a velocity measurement (which is certainly less practical). It also suggests that the lift is a high-quality measurement which provides a sufficiently rich summary of the entire wake, and should therefore serve well as a measurement strategy for feedback flow control purposes.

DYNAMIC ESTIMATION OF THE GINZBURG-LANDAU EQUATION

In this section we study the estimation problem for a simpler system: the Ginzburg-Landau equation, which is a relatively well-studied model system, and which displays many of the phenomena seen in fluid systems. This allows us to precisely quantify the efficacy of the estimator as the disturbance characteristics and measurement type vary, providing important information concerning the estimation problem with greater ease than could be achieved using direct numerical simulations of the cylinder wake.

The parallel Ginzburg-Landau equation, defined on the infinite interval, $-\infty < x < \infty$, is

$$\frac{\partial q}{\partial t}(x,t) = \left(-\nu\frac{\partial}{\partial x} + \gamma\frac{\partial^2}{\partial x^2} + \mu(x)\right) q(x,t), \qquad (6)$$

with boundary conditions $q(x,0) = q_0(x)$. and $q(x,t) < \infty$ as $x \to \pm\infty$. For a nice review of the Ginzburg-Landau equation and its use for flow control studies, see Bagheri *et al.* (2009). The convective and the dissipative nature of the flow are represented by the complex terms $\nu = U + i2c_u$ and $\gamma = 1 + ic_d$, respectively. The governing equation is of convection-diffusion type with an extra real-valued term $\mu(x) = \mu_0 - c_u^2 + \mu_2 x^2/2$ to model exponential instabilities. The parameters chosen are $U = 2.0$, $c_u = 0.2$, $c_d = -1.0$, $\mu_0 = 0.38$ and $\mu_2 = -0.01$ which are the same as those used in the subcritical (i.e. globally stable) cases considered in Bagheri *et al.* (2009) and in Chen & Rowley (2011). For these parameter values the flow is convectively unstable for $x_{\rm I} < x < x_{\rm II}$, with $x_{\rm I} = -8.25$ and $x_{\rm II} = +8.25$. This means that perturbations grow in this region as they convect downstream, but that globally the flow is stable.

The governing equation (6) is discretized using a spectral Hermite collocation method described in Bagheri *et al.* (2009). Like the cylinder, the specific type of estimator used is a Kalman filter. Our particular interest in this section is on the effect of the location of a single disturbance on the fidelity of the estimate obtained by an estimator.

Sensing is provided by a single sensor centred at $x_s = 0$. We keep the single sensor fixed at this location but, motivated by the results of the previous section, we look at two different *types* of sensor. Rather than measure $q(x,t)$ at a point, the sensor measures a weighted integral of $q(x,t)$ so that the output, $y(t)$ is given by

$$y(t) = \int_{-\infty}^{\infty} q(x,t)\exp\left(-\frac{(x-x_s)^2}{\sigma^2}\right)\mathrm{d}x + n(t) \qquad (7)$$

Two types of sensor are considered: both are centred at zero so that $x_s = 0$ in (7). The first is a 'local' sensor, for which σ in (7) is small ($\sigma = 0.4$), making the Gaussian weighting function narrow, so that a localized velocity is measured. The second is an 'integral' sensor, for which σ is large ($\sigma = 14.1$), making the Gaussian weighting much wider so that a more global, integral measure of the velocity is obtained. This second sensor type is intended to mimic the measurement of the lift seen in the previous section and is motivated by the good results achieved there.

A single disturbance (which has zero-mean, Gaussian statistics in time) acts at x_w. The position, x_w of this disturbance is varied between $-16.0 < x_w < 16.0$. These limits correspond to approximately twice the region over which perturbations grow, i.e. x_w satisfies $2x_{\rm I} < x_w < 2x_{\rm II}$.

We now present results for the two sensor types as the disturbance location varies. The estimator performance is quantified by the 2-norm of the error dynamics, $e(t) =$

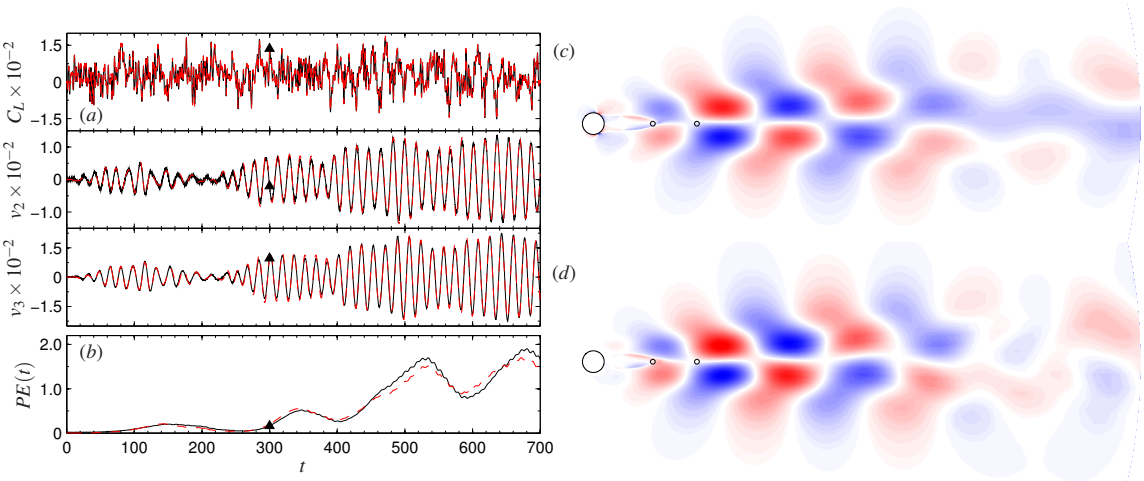

Figure 5. Estimation of the cylinder wake at $Re = 45$ using the lift coefficient: legend same as figure 3, but note that in (*a*) the lift coefficient, C_L, is plotted in place of v_1.

$\hat{q}(t) - q(t)$, defined in (3):

$$||e||_2 = \left(\int_0^\infty \int_{-\infty}^\infty e^2(x,t)\,\mathrm{d}x\,\mathrm{d}t \right)^{1/2}. \tag{8}$$

(This can be calculated straightforwardly in the frequency domain using Parseval's theorem.) We will also want to normalize this error by the 2-norm of q, obtained by replacing $e(x,t)$ by $q(x,t)$ in (8). This makes for a fairer comparison, since $||e||_2$ could change in size simply by virtue of $||q||_2$ changing in size as the disturbance location varies.

Figure 6 compares the quantities $||e||_2^2$ and $||e||_2^2/||q||_2^2$ for the two sensor types as the disturbance location, x_w, varies. The disturbance location varies between $x_w = -16.0$ and $x_w = +16.0$. We see that the local sensor outperforms the integral sensor when the disturbance occurs upstream of their centres (at $x_s = 0$), but that the integral sensor performs comparably in these cases. We also see a small range of disturbance locations (approximately $0.5 < x_w < 3.5$) for which the integral sensor outperforms the local sensor. This is explained physically by the fact that, for these values of x_w, the disturbance is entering *downstream* of the local sensor, which therefore receives little information about it, and is not able to estimate its effect on the flow. The *integral* sensor, on the other hand, receives aggregate information over a range of spatial locations, and is therefore less affected by the disturbance occurring further downstream.

We finish this section by looking in more detail at two of the cases plotted in figure 6. We do this by simulating the model in time, and then comparing the estimates obtained by the local and integral sensors. Before presenting the results we must first define the perturbation energy, $PE(t)$, and the 'energy' of the estimation error, $\Delta(t)$, since these quantities will once again be plotted. They are

$$PE(t) = \frac{1}{2}\int q^2(x,t)\,\mathrm{d}x \tag{9a}$$

$$\Delta(t) = \frac{1}{2}\int [\hat{q}(x,t) - q(x,t)]^2\,\mathrm{d}x. \tag{9b}$$

The first case we consider is $x_w = -8.5$ for which, from figure 6, the local sensor outperforms the integral sensor. The comparison in time is shown in figure 7. In parts (*a-d*) we see that both sensor types perform well, with good approximations of the flow field and $PE(t)$ being obtained in both cases. The differences between the two sensor types is seen most clearly in (*e*), which compares $\Delta(t)$ (see Eq. 9b) for the two cases. We see that the local sensor outperforms the integral sensor, which is consistent with figure 6.

The second case we consider is $x_w = 1.6$ for which, from figure 6, the integral sensor outperforms the local sensor. The comparison in time is shown in figure 8. This time the estimates for the two sensor types are not nearly as good as those obtained in figure 7. (Notice also that the amplitudes of the energies involved are now much smaller, since the disturbance is amplified over a shorter part of the domain.) We see this time that the integral sensor outperforms the local sensor—which is again consistent with figure 6—but both sensor types display difficulty in forming an accurate estimate for this more challenging case.

CONCLUSIONS

The estimation problem has been considered for two systems. First, estimation of the cylinder wake at $Re = 45$ has been considered. Excellent results have been obtained using a single velocity sensor in the wake. The accuracy

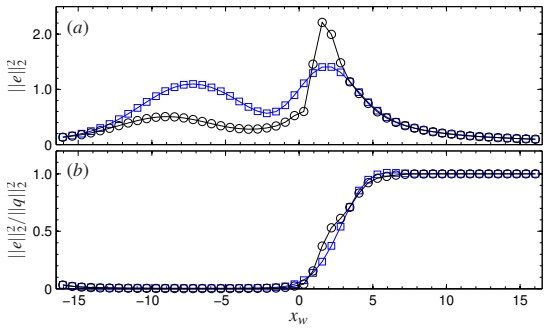

Figure 6. 2-norm of the error dynamics as a function of the disturbance location, x_w: (*a*) $||e||_2^2$; and (*b*) $||e||_2^2/||q||_2^2$. The norm for the localized sensor (black circles) is compared to that for the integral sensor (blue squares).

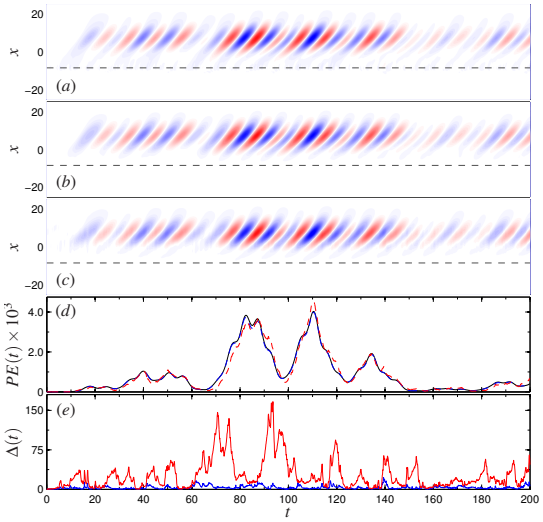

Figure 7. Estimation of the Ginzburg-Landau equation for $x_w = -8.5$: (a) the true field, $q(x,t)$; and its estimate, $\hat{q}(x,t)$ using (b) the local sensor; and (c) the integral sensor. (d) compares the true perturbation energy (black) with its estimate using the local sensor (blue) and the integral sensor (red). (e) compares $\Delta(t)$ (see Eq. 9b) for the two cases. The disturbance location is indicated ($--$) in (a-c).

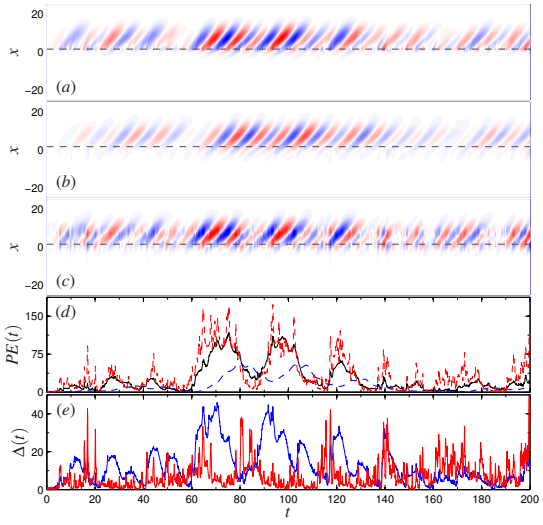

Figure 8. Estimation of the Ginzburg-Landau equation for $x_w = 1.6$: legend same as in figure 7.

of the estimate is broadly similar for the three sensor locations considered, with the sensor furthest downstream performing the best at this Reynolds number. Estimation using measurement of the lift force only has also been considered and, again, excellent results were obtained. This suggests that a more global (and surface-based) measurement such as lift provides a sufficiently rich summary of what is happening in the entire wake, and should therefore serve well as a measurement for feedback control purposes.

Second, estimation of the Ginzburg-Landau equation has been considered. The particular focus was on the accuracy of the estimate for two different sensor types: *i*) a local sensor, and *ii*) an integral sensor. This was studied by comparing the estimate from the two sensor types as the location of a single disturbance region was varied. The results show that both sensor types perform well when the disturbance is upstream of their centres, with the local sensor performing better than the integral sensor. When the disturbance occurs downstream of the sensors' centres, though, the local sensor exhibits a significant degradation in performance, and the integral sensor outperforms it.

The author would like to thank Hiroshi Naito and Koji Fukagata for helpful discussions concerning the DNS code.

REFERENCES

Adrian, R. J., Jones, B. G., Chung, M. K., Hassan, Y., Nithianandan, C. K. & Tung, A. T.-C. 1989 Approximation of turbulent conditional averages by stochastic estimation. *Phys. Fluids* **1** (6), 992–998.

Anderson, B. D. O. & Moore, J. B. 1979 *Optimal filtering*. Prentice Hall.

Bagheri, S., Henningson, D. S., Hoepffner, J. & Schmid, P. J. 2009 Input-output analysis and control design applied to a linear model of spatially developing flows. *Applied Mech. Rev.* **62** (2), 020803.

Chen, K. K. & Rowley, C. W. 2011 $\mathscr{H}_2$ optimal actuator and sensor placement in the linearised complex Ginzburg-Landau system. *J. Fluid Mech.* **681**, 241–260.

Fukagata, K. & Kasagi, N. 2002 Highly energy-conservative finite difference method for the cylindrical coordinate system. *J. Comput Phys.* **181** (2), 478–498.

Guezennec, Y. G. 1989 Stochastic estimation of coherent structures in turbulent boundary layers. *Phys. Fluids* **1** (6), 1054–1060.

Guzmán Iñigo, J., Sipp, D. & Schmid, P. J. 2014 A dynamic observer to capture and control perturbation energy in noise amplifiers. *J. Fluid Mech.* **758**, 728–753.

Hœpffner, J., Chevalier, M., Bewley, T. R. & Henningson, D. S. 2005 State estimation in wall-bounded flow systems. Part 1. Perturbed laminar flows. *J. Fluid Mech.* **534**, 263–294.

Illingworth, S. J., Morgans, A. S. & Rowley, C. W. 2011 Feedback control of flow resonances using balanced reduced-order models. *J. Sound Vib.* **330**, 1567–1581.

Juang, J. 1994 *Applied System Identification*. Prentice Hall.

Julier, S. J. & Uhlmann, J. K. 2004 Unscented filtering and nonlinear estimation. *Proc. IEEE* **92** (3), 401–422.

Kalman, R. E. 1960 A new approach to linear filtering and prediction problems. *J. Basic Eng.* **82** (1), 35–45.

Ma, Z., Ahuja, S. & Rowley, C. 2009 Reduced order models for control of fluids using the Eigensystem Realization Algorithm. *Theor. Comp. Fluid Mech.* **25**, 233–247.

Rowley, C. W. & Juttijudata, V. 2005 Model-based control and estimation of cavity flow oscillations. *44th IEEE Confer. Decis. Contr.* **15**, 512–517.

Williamson, C. H. K. 1989 Oblique and parallel modes of vortex shedding in the wake of a circular cylinder at low Reynolds numbers. *J. Fluid Mech.* **206**, 579–627.

Williamson, C H K 1996 Vortex dynamics in the cylinder wake. *Annu. Rev. Fluid Mech.* **28**, 477–539.